

# Laser microdissection coupled with RNA-seq reveal cell-type and disease-specific markers in the salivary gland of Sjögren's syndrome patients

M. Tandon<sup>1,2</sup>, P. Perez<sup>1</sup>, P.D. Burbelo<sup>3</sup>, C. Calkins<sup>2</sup>, I. Alevizos<sup>1</sup>

<sup>1</sup>*Sjögren's Syndrome and Salivary Gland Dysfunction Unit, National Institutes of Health, National Institute of Dental and Craniofacial Research, Bethesda, MD, USA;*

<sup>2</sup>*Department of Microbiology and Immunology, Jefferson College of Biomedical Sciences, Thomas Jefferson University, Philadelphia, PA, USA;*

<sup>3</sup>*Dental Clinical Research Core, National Institute of Dental and Craniofacial Research, Bethesda, MA, USA.*

---

## Abstract

### Objective

*Little is known about the molecular details regarding the contribution of different cell types of the salivary gland to the altered gene expression profile seen in Sjögren's syndrome (SS).*

---

### Methods

*Using laser microdissection, tissue samples enriched in acini, ducts and inflammatory foci in subjects with and without SS were isolated for RNA-seq analysis. Gene expression profiles were analysed and selected enriched genes were further examined using real time PCR and by immunofluorescence.*

---

### Results

*RNA-seq analysis of salivary biopsies from subjects with and without SS revealed marked differences in gene expression occurring in the ductal and infiltrating cells compared to acinar cells. Up-regulated genes in the SS ductal cells included C4A complement and the SLC26A9 ion channel. The inflammatory infiltrate showed the most dramatic differences in gene expression and contained up-regulated genes associated with T-cells, natural killer, dendritic and basophils/mast cells. qPCR with total salivary gland mRNA confirmed the differential mRNA expression of several genes (MMP9, FOL1HB, CCL21, CCR7), thereby validating the approach. Additional immunofluorescence studies demonstrated high expression and co-localisation of CCL21 chemokine and CCR7 chemokine receptor within the SS infiltrates.*

---

### Conclusion

*Major gene expression changes in the salivary gland of SS were detected in the ductal and inflammatory cells and not in the acinar cells. Two chemokines involved in immune cell trafficking to secondary lymphoid tissue, CCR7 and CCL21, showed markedly increased expression and may contribute to the recruitment of diverse immune cells to the salivary glands, causing inflammation and loss of secretory function.*

---

### Key words

acini, ducts, RNA-seq, laser microdissection, salivary gland, Sjögren's syndrome

Mayank Tandon, BS  
Paola Perez, PhD  
Peter D. Burbelo, PhD  
Catherine Calkins, PhD  
Ilias Alevizos, DMD, PhD

Please address correspondence to:

Dr Ilias Alevizos,  
MPTB, NIDCR, NIH,  
Building 10, Room 1N110, MSC-1190,  
Bethesda, MD 20892 USA.  
E-mail: alevizosi@mail.nih.gov

Received on December 23, 2016; accepted  
in revised form on January 25, 2017.

© Copyright CLINICAL AND  
EXPERIMENTAL RHEUMATOLOGY 2017.

## Introduction

Autoimmune diseases are complex pathologies of the immune system that are thought to be influenced by both genetic and environmental interactions. Primary Sjögren's syndrome (SS), characterised by salivary and ocular dryness, is one of most common autoimmune diseases, which primarily targets exocrine tissue leading to glandular dysfunction. One of the main diagnostic criteria for SS is focus score, a quantitation of the number of infiltrates, which are often described to be co-localised with ductal structures by histological analysis (1, 2). Although many SS patients demonstrate salivary and ocular inflammation and harbour autoantibodies against the SSA and/or SSB autoantigens, a mechanistic understanding of the disease is elusive (3). Recent studies demonstrate that many SS patients have evidence of chronic immune activation as per the presence of autoantibodies years before clinical onset (4). However, the factors and cell types triggering immune activation are unknown, and they are likely to involve environmental stimuli including infectious agents. Evidence for an additional genetic component in SS comes from genome-wide association studies that have identified multiple genes linked to immune activation including HLA, IRF-4 immune transcription factor, and B-cell signalling molecules (5-7). Immune activation and trafficking have also been suggested as potential therapeutic targets, particularly the mechanisms and genes involved in tertiary lymphoid structure formation in SS salivary glands (8).

Analysis of gene expression changes in SS has also provided important information for understanding pathogenesis. A study by Gottenberg *et al.*, 2006 employed a 5000 gene microarray to probe mRNA changes from whole salivary gland biopsies (9). One major finding of this study was evidence for the presence of an interferon-alpha gene signature in the salivary gland from SS patients. The cytoplasmic sensors TLR-8 and TLR-9 were two of the up-regulated genes identified, and were further found to be enriched in dendritic cells within ectopic germinal centers in patient salivary glands. Similar findings

by several other groups employing gene arrays have also examined gene expression changes in the salivary gland and even peripheral blood, which have yielded evidence of immune activation (10-18). However, cell-type-specific contributions to the changes in gene expression have not been evaluated because whole salivary gland tissue or peripheral blood mononuclear cells was used for RNA extraction in all previous studies.

RNA-seq is among the highest resolution methods to study gene expression (19). Here, we applied laser microdissection (LMD) to obtain three different cell populations, acini, ducts and inflammatory infiltrates, from minor salivary gland biopsies of SS patients and healthy controls (HC) for RNA extraction and subsequent gene expression profiling using RNA-seq. Analysis of the cell-type-specific transcriptomes identified many new genes exhibiting altered gene expression and confirming many previous findings, as well as provide new cell-type and SS-specific markers. Most importantly, these findings highlight the fact that changes in gene expression in ductal and inflammatory cells are able to better segregate patient from healthy tissue.

## Materials and methods

### Patient selection

The studies were conducted according to the principles expressed in the Declaration of Helsinki. Informed written consent was obtained from all subjects in accordance with the guidelines of the Department of Health and Human Services under NIDCR IRB-approved protocols. Minor salivary gland biopsies were obtained from consenting healthy controls and primary SS patients. The healthy controls were Caucasian, females, and negative for the SS specific autoantibodies (anti-SSA and anti-SSB). The SS subjects fulfilled the American-European criteria for classification for primary SS, were all females, Caucasian, anti-SSA autoantibody positive, and had a positive biopsy with a low focus score (*i.e.* 1-3). We chose SS patients with focus scores less than 4 in order to maximise our ability to collect intact acini and

Funding: this research was supported by the Intramural Research Program of the National Institutes of Health (NIH), National Institute of Dental and Craniofacial Research.

Competing interests: none declared.

ducts and as such, likely represent SS subjects in early stages of disease progression.

#### *Laser microdissection (LMD)*

PEN membrane slides (Leica Microsystems) were soaked with RNase Away (Molecular BioProducts, catalogue #7000), air-dried, and then treated with UV light at 254 nm for 30 minutes. OCT blocks with minor salivary gland biopsies were then sectioned into two 7 µm slices per slide under RNase-free conditions and kept at -80° C. Each slide was fixed and stained using the following incubations in disposable Pap jars: 75% ethanol (2 minutes), DEPC water (30 seconds), repeat DEPC wash, haematoxylin (15 seconds), DEPC wash (30 seconds), Scott's Tap Water Substitute (15 seconds), DEPC water (30 seconds), eosin (15 seconds), 95% ethanol (15 seconds), 100% ethanol (30 seconds), repeat 100% ethanol. After 5 minutes of air drying, the slides were imaged and dissected on the Leica AF 6000 LX Leica AMS-LMD microscope and the Leica LMD software.

#### *RNA isolation*

Microdissected pieces of the tissue sections were collected in lysis buffer provided with the Norgen RNA/DNA/Protein Purification Plus Micro Kit (Norgen Biotek Corp.) and were used for isolated of RNA, DNA, and protein. RNA was quantified using the RNA Pico 6000 Kit on the Bioanalyzer 2100 instrument (Agilent Technologies). For whole minor salivary gland biopsies mounted in OCT, ten 20 µm thick slices were isolated using the miRCURY RNA Isolation Kit for Tissue (Exiqon). The protocol was modified for sliced tissue by passing the sample through a 25-gauge needle 5–10 times after the lysis buffer was added.

#### *RNA sequencing*

RNA-seq libraries were created using the Ion AmpliSeq™ Transcriptome Human Gene Expression Kit (Thermo Fisher Scientific) using 1–10 ng input RNA. This kit provides pre-designed primers for 20,802 genes that yield 70–115 bp amplicons for each gene. Template preparation was performed

using the Ion PI™ IC 200 Kit (Thermo Fisher Scientific) and sequenced using the Ion PI™ Sequencing 200 Kit v. 3 (Thermo Fisher Scientific) for the Ion Proton platform.

#### *Data analysis*

The Torrent Suite 4.4.2 pipeline was used for primary analysis and read mapping using the Torrent Mapper (TMAP) aligner. Raw read counts were normalised using the ampliSeqRNA v. 4.4.2.1 analysis plugin, which outputs reads per million (RPM) values for each gene, and used to generate a global PCA plot to identify outlier samples. Raw read counts for the filtered dataset were used for further analysis. Genes with an average raw count of less than one were removed and the remaining were input for differential expression testing using the DESeq2 package (20) for the R statistical programming language. Reported *p*-values are from gene-wise Student's *t*-tests. Gene set enrichment analysis (GSEA) was performed using the web tools provided by the Broad Institute by computing overlaps with the 'Hallmark' and 'Motif' gene sets in the Molecular Signature Database (<http://software.broadinstitute.org/gsea/msigdb/search.jsp>) (21).

#### *Real-Time Quantitative PCR*

Total RNA (10 ng) from whole minor salivary gland biopsies of an independent group of four healthy controls and four SS subjects was used to make cDNA using the SuperScript VILO cDNA Synthesis Kit (Thermo Fisher). Quantitative real-time reverse transcription PCR (RT-PCR) was performed using Taqman Master Mix (Applied Biosystems) and Taqman probes for MMP9, FOLH1, SNX22, CCR7, CCL21, SLC26A9, and GAPDH. All RT-PCR experiments were performed on StepOnePlus PCR instrument and analysed using the accompanying StepOnePlus Software v. 2.3 (Applied Biosystems), which calculates fold changes based on the  $2^{-\Delta\Delta Ct}$  method (22).

#### *Immunofluorescent staining*

Formalin-fixed paraffin embedded minor salivary gland biopsies from patients (n=4) and healthy controls

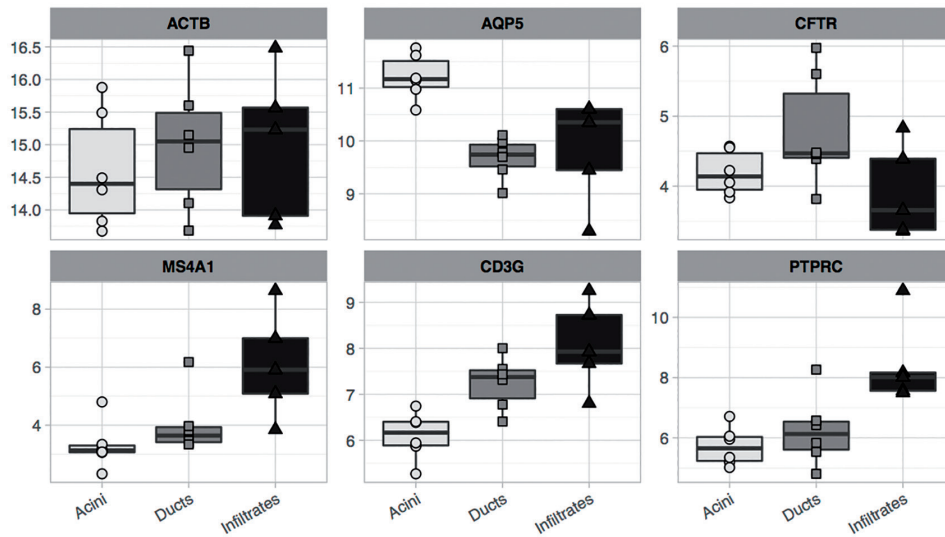
(n=4) were sectioned in 7 µm slices. Slides were deparaffinised by warming to 60°C for 15 minutes and then washing in xylene, ethanol, and water, as described previously (23). Antigen retrieval was performed by bathing the slides in 0.01 M Citric acid buffer pH 6.0, placing them inside a pressure cooker and in a microwave oven for 15 minutes (24). The slides were then washed in 1X PBS three times over 15 minutes and incubated in a 100 mM Glycine solution for 20 minutes. The tissue was incubated in a blocking buffer (10% FBS, 0.4% saponin, 0.02% azide in 1X PBS) for 60 minutes, and subsequently washed in 1X PBS 3 times over 15 minutes. Primary antibodies were incubated in blocking buffer at 4° C overnight for SLC26A9 (Sigma, dilution 1:100, rabbit host) and for 2 hours at room temperature for CCL21 (Sigma, dilution 1:250, rabbit host). The slides were then incubated with fluorescent secondary antibodies (Jackson ImmunoResearch), diluted 1:200 in blocking buffer, directed at the host species of the primary antibodies for one hour at room temperature and subsequently washed in 1X PBS containing 0.2% Triton X-100 (PBS-T). The CCR7 antibody (Abcam, dilution 1:100, rabbit host) was directly labelled with the Zenon Rabbit IgG Labeling Kit (Thermo Fisher) and applied to tissue sections for 2 hours at room temperature after indirect labelling of CCL21, followed by washing in PBS-T. Slides were dried and mounted in ProLong Diamond Antifade Mountant with DAPI (Thermo Fisher). Slides were imaged using an Olympus BX61VS motorised slide scanner microscope (Olympus Life Science).

## **Results**

### *Gene expression patterns elucidated by RNA-seq are different in acinar, ductal and inflammatory cells*

Minor salivary gland biopsies were dissected from five healthy controls and five patients with primary SS (see Methods for patient details) using LMD. RNA isolates from these biopsies were used to prepared libraries using the Ion AmpliSeq™ Transcriptome Human Gene Expression Kit and then

1A)



1B)

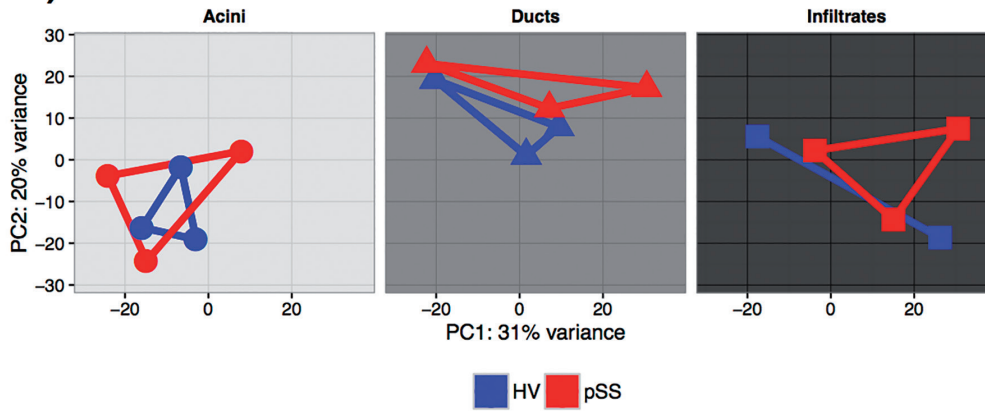


**Fig. 1.** Distinct gene expression profiles between acini, ducts and infiltrate in the salivary gland of healthy controls and SS subjects.

**A.** Expression of known cell type-specific markers in the LMD data. ACTB is a housekeeping gene, AQP5 and CFTR are acinar and ductal specific markers respectively, and MS4A1 (CD20), CD3G (CD3 gamma subunit), and PTPRC (CD45) are inflammatory cell markers.

**B.** Principal component analysis of the transcriptomic profile in three cell types for healthy and SS subjects. PCA was computed using the 500 genes with highest variance across the entire dataset. PC1 and PC2 are graphed showing samples from acini, ducts, and infiltrate with blue and red colouring indicating healthy controls (HC) and SS samples, respectively. As shown, the PCA profile of the acini samples from three HC and SS overlapped. In contrast, the ductal (from 3 HC and 3 SS) and infiltrate (2 HC and 3 SS) samples showed non-overlapping PCA profiles.

sequenced on the Ion Proton sequencing platform (Life Technologies). The RNA-seq data were pre-processed (see *Methods*) to remove outlier samples and lowly expressed genes, leading to the analysis of 16,849 genes in six samples each for acini and ducts (three SS and three HCs in both groups), and five infiltrate samples (three SS and two HCs). The mRNA isolated from acini, ducts, and immune infiltrates were enriched for known cell-type markers in the salivary gland. As expected, ACTB, a ubiquitously expressed mRNA for beta-actin, showed relatively similar mRNA levels in the three different cell fractions (Fig. 1A). In contrast, AQP5, an acinar cell marker and CFTR, a known channel in ducts, showed significant mRNA enrichment in the acini and ductal tissues, respectively. Additionally, MS4A1, CD3G, and PTPRC, markers for B-cells, T-cells, and mono-

cytes, respectively, exhibited marked upregulation in the isolated infiltrate fraction.

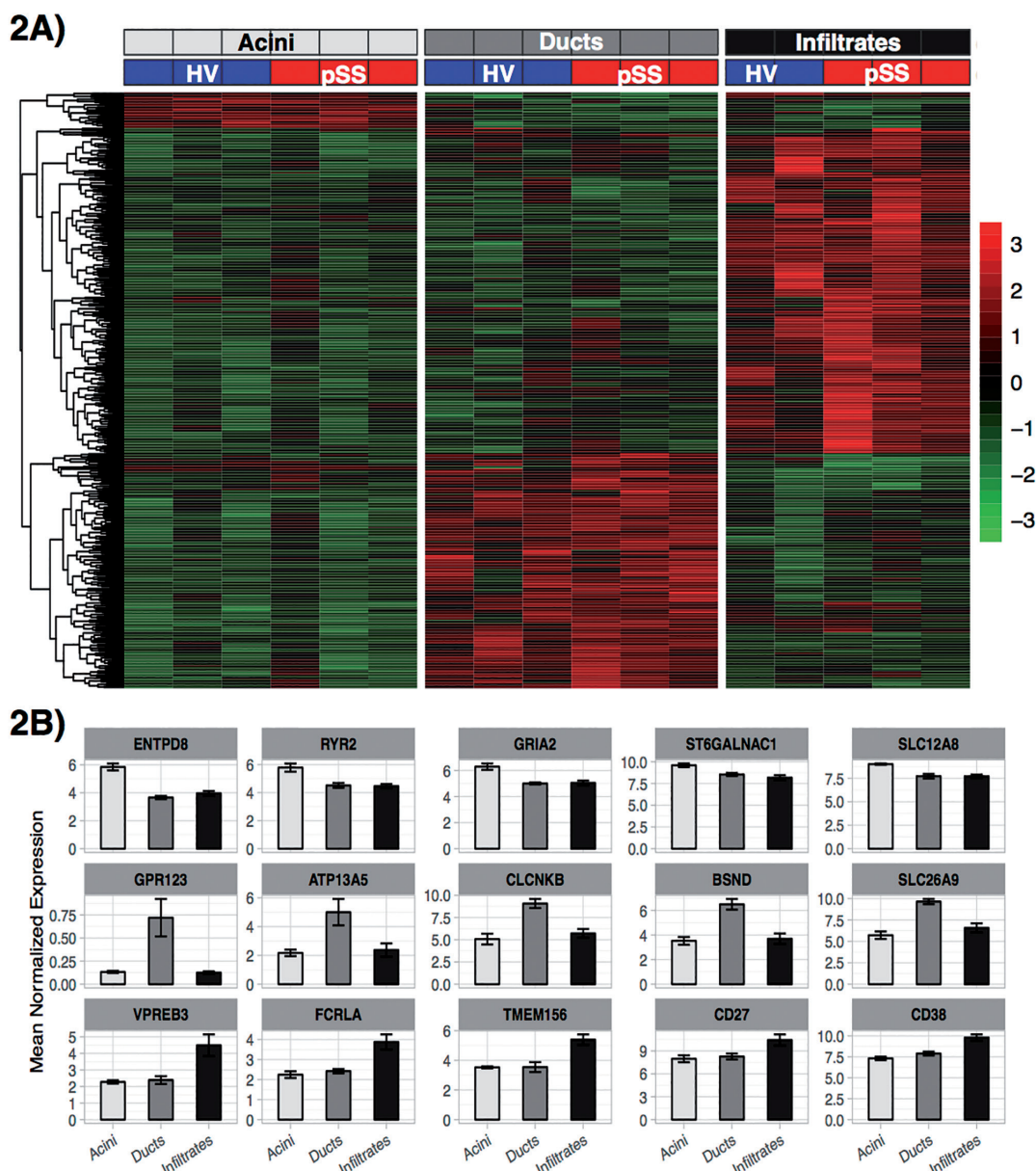
Principal components analysis (PCA), an unsupervised method for visualisation and analysis of high dimensional data, was used to determine if the cell groups could be phenotypically separated based on the RNA-seq expression data. Using the top 500 genes with the greatest variance in the dataset, the first two principal components (PCs) were computed and determined to account for 51% of the total variance in the data. A plot of PC1 versus PC2 demonstrated that gene-based clustering could separate the three distinct cell types in an unsupervised manner (Fig. 1B). However, only the ductal and infiltrate samples showed a clear separation between the SS and healthy group, while the acinar profiles were largely overlapping and grouped the healthy

and SS samples together. One interpretation of this finding is that there are more significant SS-specific changes in gene expression in the ductal and inflammatory cells compared to acini, which may help explain the persistent periductal localisation of infiltrates that is classically described in SS (25, 26). Differential expression analysis of the LMD data for cell-type enriched genes revealed 469 differentially expressed genes ( $p < 0.0001$ ), which were visualised for expression as a heatmap with hierarchical clustering of genes (Fig. 2A). Some of the novel cell type-enriched mRNAs in this gene set included ENTPD8 and RYR2 in acini and GPR123 and SLC26A9 in ductal cells (Fig. 2B). In the immune infiltrate, mRNA enrichment of VPREB3, CD27, and CD38 showed the presence of a mixed population of both B-cells and T-cells in various stages of maturity (Fig. 2B).

**Fig. 2.** Differential gene expression analysis reveals cell-type enriched genes.

**A.** Heatmap of 469 differentially expressed genes chosen based on  $p < 0.0001$  in one cell type regardless of disease status. Colours are scaled by row and the scale represents standard deviation above or below the mean normalised expression for each gene.

**B.** RNA-seq expression values showing differential expression of selected genes in acini, ducts and infiltrate. Barplots show regularised log transformation expression values with error bars for standard error.



### Marked gene expression changes are associated with the ductal cells and inflammatory infiltrate in SS

Differential expression analysis was also used to identify genes enriched in the three tissues of SS biopsies relative to HC biopsies (Fig. 3A). Interestingly, a heatmap of the acinar fraction showed minimal differences in gene expression between the healthy controls and SS subjects. In contrast, the ductal and infiltrate fractions showed more dramatic and consistent differences in gene expression (Fig. 3A). Further illustrations of some of the specific differentially expressed SS genes are listed in Fig. 3B. As shown, there were relatively similar

levels of ACTB in SS as the controls in the three cell types. In acinar samples, there was less RYR2 receptor expression in SS than in controls (Fig. 3B). Similarly, there was a drop in expression of MPO and CDH12 in SS compared to controls. However, there was increased expression of C4A in the SS ductal fractions, and IFNA21 and TLR8 expression were elevated in the infiltrate fraction (Fig. 3B). Moreover, the immune infiltrate of SS contained many other up-regulated genes associated with T-cells, natural killer, dendritic and basophils/mast cells. Further analysis by Gene Set Enrichment Analysis (GSEA) for identifying affected pathways

showed enrichment of broadly relevant cell signalling such as antigen processing and presentation, as well as several transcription factors (data not shown). Of the mRNAs up-regulated in SS patient infiltrates, 27 genes contained the binding motif for the transcription factor ETS2 in their promoter region, which has been shown to be important in immune responses against herpes viruses like Epstein-Barr virus (EBV) (27) and Hepatitis B (HBV) (28, 29). Although the biological relevance of this finding is not immediately clear, there is a history of associations between EBV and SS (30-32), and our data provide a possible mechanism through ETS2.

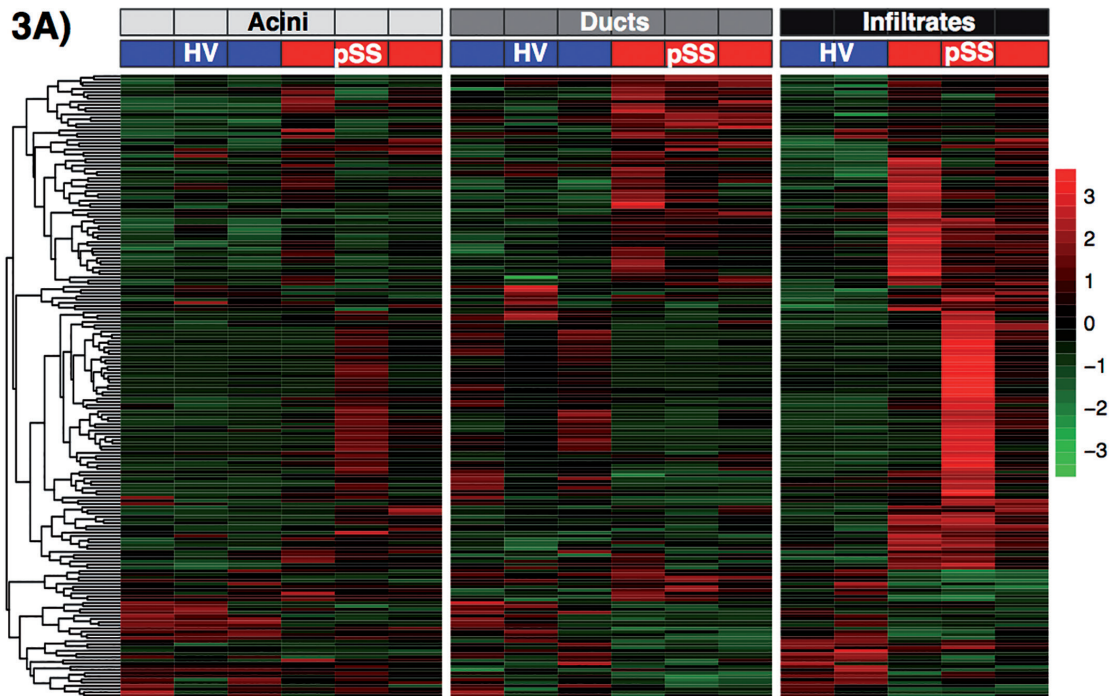
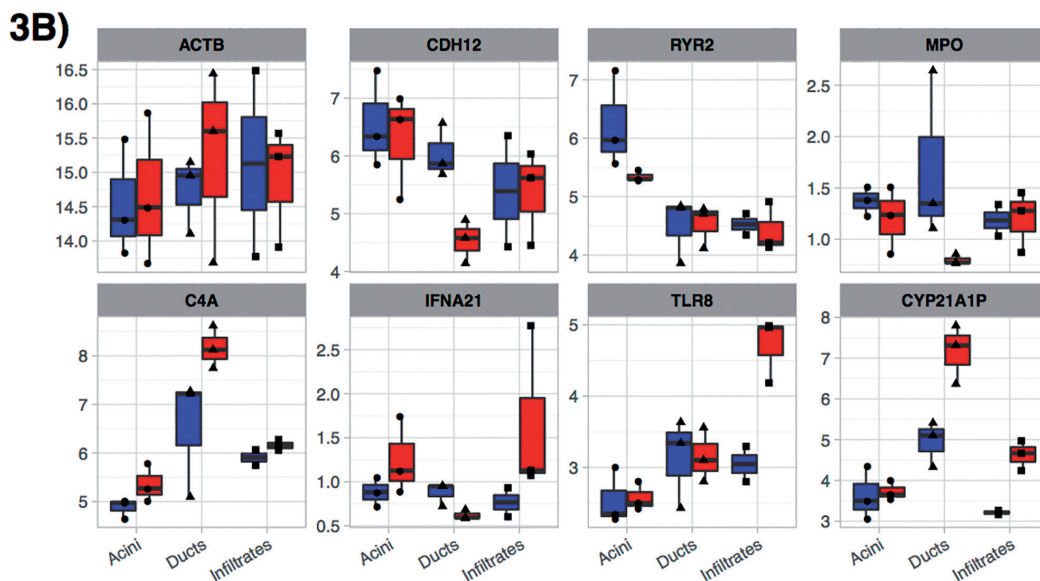


**Fig. 3.** SS-specific transcriptomic profiles generated in acinar, ductal, and infiltrate fractions.

**A.** Heatmap of 195 differentially expressed genes ( $p < 0.01$ ) in SS patients in at least one cell type. Colours are scaled by row and the scale represents standard deviation above or below the mean expression for each gene.

**B.** Barplots of selected SS-enriched and cell-type-specific markers showing the values normalised by the regularised log transformation and error bars for standard error.



*Confirmation of differential SS-expressed genes Identified by RNA-seq*  
 Our approach of coupling LMD with RNA-seq uncovered a treasure trove of novel genes showing differential SS gene expression. To further validate these findings, selected genes showing differential genes expression in SS were measured using qPCR. Since the amount of RNA extracted by LMD from tissue was too low for reliable quantitation by qPCR, we utilised RNA extracted from whole minor salivary gland biopsy samples from an independent cohort of four healthy controls

and four SS patients. For these confirmation experiments, we first studied the differential gene expression of two genes, MMP9 and FOL1HB, which were the most highly up- and down-regulated genes, respectively, in all three cell types in SS patients (Fig. 4A). qPCR analysis of MMP9 and FOL1HB showed complete concordance with the LMD data (Fig. 4B). Additionally, SNX22, another disease-related significantly differentially expressed genes, showed a modest increase in SS only in the infiltrate fraction (Fig. 4A). This cell-type specificity, which is diluted

out by RNA from additional cell types, is likely why the qPCR assay on whole biopsy RNA shows only a small, non-significant upregulation (Fig. 4B).

To extend our studies to the confirmation of both differential mRNA and protein expression, we examined three additional biologically relevant targets, CCR7, CCL21, and SLC26A9. CCR7 is a chemokine receptor most commonly associated with T-cells that binds to the chemokine CCL21, and together they are involved in immune trafficking to secondary lymphoid organs (33, 34). SLC26A9 is an ion channel known

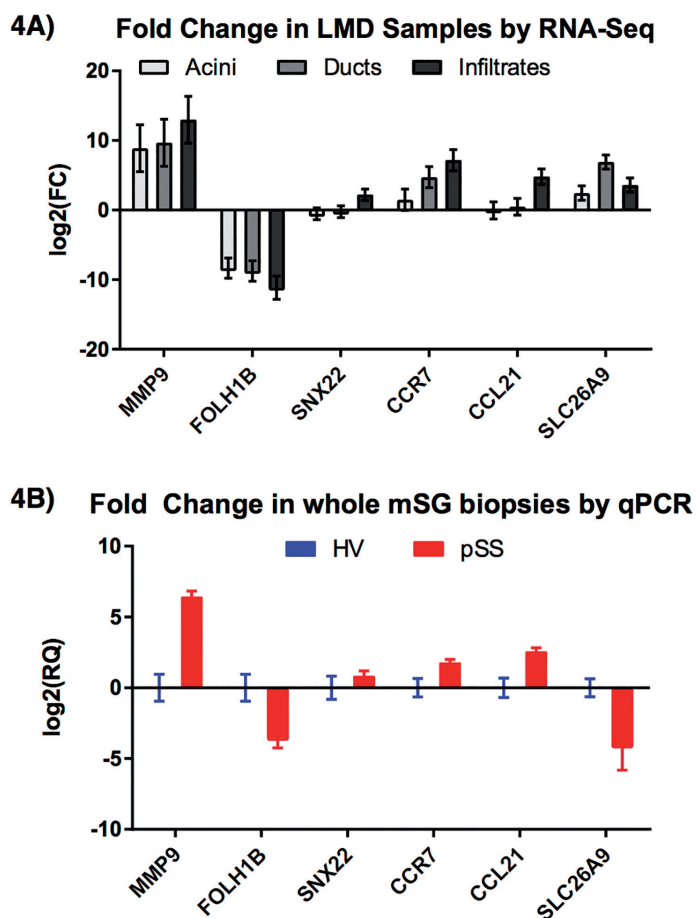


**Fig. 4.** RNA expression level of selected genes in microdissected samples by RNA-seq compared to qPCR analysis of biopsy of whole minor salivary gland. A. Cell-type specific fold-changes in gene expression by RNA-seq of selected genes in SS patients over healthy controls. Bars show log<sub>2</sub> transformed fold changes and standard error.

B. Fold-changes in patients of the same genes determined by qPCR on RNA derived from whole minor salivary gland biopsies. Data shown are log<sub>2</sub> transformed relative quantitation (RQ) values computed using healthy controls as the reference group and GAPDH as a housekeeping control. Error bars show 95% confidence interval.

to associate with CFTR (35-38). As shown by the RNA-seq data, CCR7 and CCL21 were marked upregulated in patient infiltrates and SLC26A9 showed the highest elevation in the SS ductal fraction (Fig. 4A). qPCR analysis of CCR7 and CCL21 demonstrated concordance with the RNA-seq results confirming the increased expression of these mRNAs in SS salivary gland (Fig. 4B). Paradoxically, the qPCR expression data for SLC26A9 mRNA did not show concordance between the two methods, demonstrating up-regulation in SS by RNA-Seq (Fig. 4A) and downregulation in SS by qPCR (Fig. 4B). Based on these differences, we postulated that the results may have been skewed by variations in the tissue sampling used for each ap-

proach. As a complementary approach, immunofluorescence was employed to examine the protein expression of CCR7, CCL21 and SLC26A9 in the minor salivary gland biopsy sections from healthy controls and SS (Fig. 5). In the healthy controls, CCL21 protein staining was observed in some ducts, but not acinar cells, which is consistent with the RNA-seq data (Fig. 5A). However in SS, there was marked overlap of CCR7 and CCL21 protein expression localising to the inflammatory infiltrate (Fig. 5B). Immunofluorescence staining for SLC26A9 also showed striking differences in protein amount and localisation between the healthy controls and SS subjects (Fig. 5C and 5D). In healthy acini, SLC26A9 was expressed at a lower level and exhibited a clas-

sical apical staining pattern similar to CFTR and consistent with its role as a chloride channel (Fig. 5C and data not shown). However, in the biopsies from SS, there was pronounced increased luminal staining of SLC26A9 in the ducts as well as in basolateral regions of acini. Thus, the protein expression patterns seen by immunofluorescence staining substantiates the mRNA expression observed by RNA-seq for CCR7, CCL21, and SLC26A9.

## Discussion

The salivary gland is a complex and heterogeneous tissue that contains multiple cell types including acinar, ductal, fibroblasts and immune cells, making it difficult to study in a disease context. To date, attempts at characterising gene alterations in SS have been limited to gene microarray approaches using unselected biopsy samples containing mixed cell types (10-17). Here we applied a different strategy coupling LMD and RNA-seq to define the global transcriptomic expression profiles of three functionally distinct cell populations, acini, ducts and infiltrate, in the salivary gland. From analysis of 16,849 genes, we found evidence for the success of this approach in the enrichment of known cell-specific genes (*e.g.* AQP-5, CFTR, CCL21) in each fraction and the ability of principal component gene analysis to differentiate between the three different cell types. Importantly, we extended this approach to examine differences in cell-type specific profiles between healthy controls and SS subjects. One major finding was that the gene expression profile of acini appeared relatively similar between healthy controls and SS. In contrast, marked gene expression alterations were detected in the ducts and infiltrates. These data support the possibility that the major pathologically driven processes in SS are occurring in the ducts and infiltrate and not in the acini.

The paucity of differential expressed acini-associated genes that we detected is also consistent with published studies in the literature. Two meta-analyses of previous gene expression studies revealed that the strongest and perhaps only point of agreement between

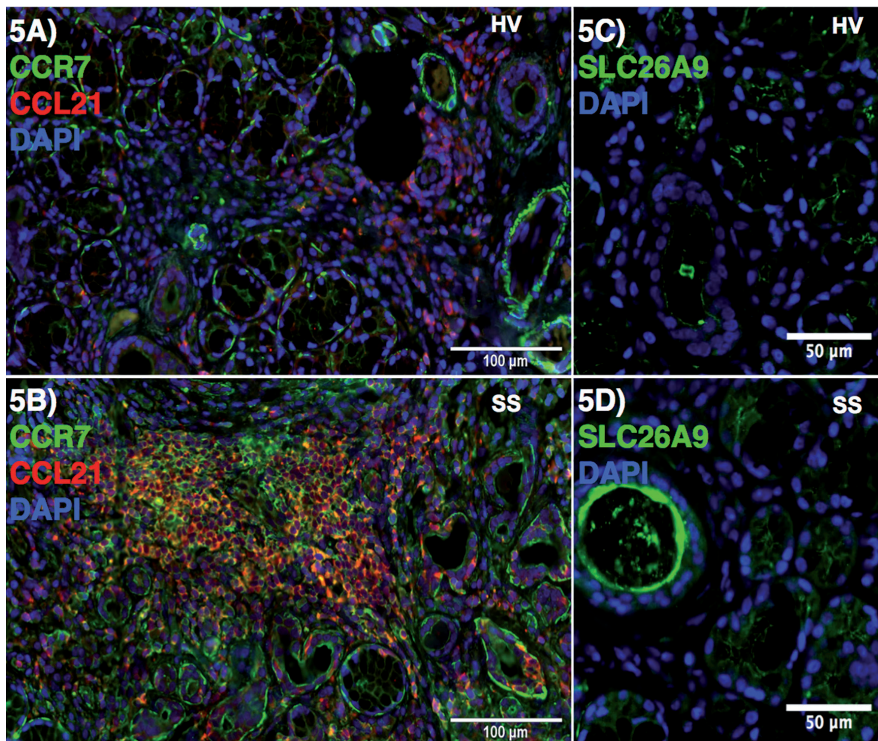


**Fig. 5.** Immunofluorescence staining of CCR7, CCL21, and SLC26A9 in the salivary glands of healthy controls and SS subjects. Representative images are shown for the immunofluorescence staining of CCR7 (green) and CCL21 (red) in the salivary biopsy of healthy controls (A) and SS (B). Similarly, SLC26A9 staining (green) is shown in the salivary biopsy of healthy volunteer (C) and SS (D). DAPI fluorescent staining is included in the images to visualise the nuclei in the sections.

them is enrichment of interferon- and immune-related genes (39, 40). Based on our own RNA-seq analysis with defined cell populations and qPCR of unfractionated salivary tissue, we believe that the lack of agreement is driven by stochastic sampling of the biopsy tissue. Nevertheless, the large number of immune-related genes up-regulated in SS detected in our study underscores the importance of the infiltrate in the dysfunction observed in the salivary gland in SS. The identification of multiple interferon-inducible genes including OAS1, IFNA2, IFNA21, and ISG15 is also consistent with the interferon-alpha signature (9, 14, 41). Moreover, we found up-regulated genes associated with T-cells, natural killer, dendritic and basophils/mast cells confirming the contribution of multiple cell types involved in the immune infiltrate. Remarkably, a study by Maehara (42), who examined the immune infiltrate by LMD and real-time PCR in SS compared to controls, found elevated mRNA expression in SS of all their preselected genes for cytokine and immune-related transcription

factors. These findings along with published gene array studies are consistent with diverse immune cell activation occurring in the SS salivary gland. Although the exact initiating event causing the accumulation of immune cells in the SS salivary gland is not known, our finding of increased mRNA and protein expression of two chemokine signalling genes, CCR7 and CCL21, may suggest their role as drivers of immune cell accumulation and inflammation. This finding is also in agreement with a recent reports showing elevated CCR7 mRNA in whole minor salivary gland biopsies of SS subjects, as well as increased staining of CCL21 at the protein level (43, 44). Further evidence for a functional role of this chemokine-chemokine receptor pair in SS pathogenesis was the increased co-staining of CCR7 and CCL21 protein in salivary biopsies of SS subjects, supporting the role of these molecules of being involved in the increased and aberrant immune trafficking seen in SS patients (33, 34). The high throughput RNA-seq dataset generated here may

be particularly beneficial for hypothesis generation and testing of additional genes involved in SS. One emerging area of focus in the pathogenesis of SS involves the loss of homeostasis in the salivary epithelium as an initiating factor in the pathogenesis of SS (45). Consistent with this hypothesis, we confirmed the increased MMP9 mRNA reported in SS (46), which is thought to cause greater proteolytic activity in SS salivary gland leading to disorganisation of the basal lamina (47). Moreover, our finding for the increased mRNA, protein expression and altered cellular localisation of SLC26A9 in SS is intriguing. This channel is involved in acid-base balance and anion homeostasis and its dysregulation may contribute to the altered ionic composition reported in SS saliva (48, 49). Further work is needed to mechanistically understand if the SLC26A9 mRNA, protein amount and localisation changes seen in SS are driven by immune mediators or some other pathological process.

## References

1. NIKOLOV NP, ILLEI GG: Pathogenesis of Sjögren's syndrome. *Curr Opin Rheumatol* 2009; 21: 465-70.
2. VITALI C, BOMBARDIERI S, JONSSON R *et al.*: Classification criteria for Sjögren's syndrome: a revised version of the European criteria proposed by the American-European Consensus Group. *Ann Rheum Dis* 2002; 61: 554-8.
3. VOULGARELIS M, TZIOUFAS AG: Pathogenetic mechanisms in the initiation and perpetuation of Sjögren's syndrome. *Nat Rev Rheumatol* 2010; 6: 529-37.
4. JONSSON R, THEANDER E, SJOSTROM B, BROKSTAD K, HENRIKSSON G: Autoantibodies present before symptom onset in primary Sjögren's syndrome. *JAMA* 2013; 310: 1854-5.
5. LI Y, ZHANG K, CHEN H *et al.*: A genome-wide association study in Han Chinese identifies a susceptibility locus for primary Sjögren's syndrome at 7q11.23. *Nat Genet* 2013; 45: 1361-5.
6. BURBELO PD, AMBATIPUDI K, ALEVIZOS I: Genome-wide association studies in Sjögren's syndrome: What do the genes tell us about disease pathogenesis? *Autoimmun Rev* 2014; 13: 756-61.
7. FANG K, ZHANG K, WANG J: Network-assisted analysis of primary Sjögren's syndrome GWAS data in Han Chinese. *Sci Rep* 2015; 5: 18855.
8. BARONE F, COLAFRANCESCO S: Sjögren's syndrome: from pathogenesis to novel therapeutic targets. *Clin Exp Rheumatol* 2016; 34 (Suppl. 98): S58-62.
9. GOTTENBERG JE, CAGNARD N, LUCCHESI C *et al.*: Activation of IFN pathways and plas-

- macytoid dendritic cell recruitment in target organs of primary Sjögren's syndrome. *Proc Natl Acad Sci USA* 2006; 103: 2770-5.
10. HJELMERVIK TO, PETERSEN K, JONASSEN I, JONSSON R, BOLSTAD AI: Gene expression profiling of minor salivary glands clearly distinguishes primary Sjögren's syndrome patients from healthy control subjects. *Arthritis Rheum* 2005; 52: 1534-44.
  11. WAKAMATSU E, NAKAMURA Y, MATSUMOTO I *et al.*: DNA microarray analysis of labial salivary glands of patients with Sjögren's syndrome. *Ann Rheum Dis* 2007; 66: 844-5.
  12. KILLEDAR SJ, ECKENRODE SE, MCINDOE RA *et al.*: Early pathogenic events associated with Sjögren's syndrome (SjS)-like disease of the NOD mouse using microarray analysis. *Lab Invest* 2006; 86: 1243-60.
  13. HORVATH S, NAZMUL-HOSSAIN AN, POLLARD RP *et al.*: Systems analysis of primary Sjögren's syndrome pathogenesis in salivary glands identifies shared pathways in human and a mouse model. *Arthritis Res Ther* 2012; 14: R238.
  14. EMAMIAN ES, LEON JM, LESSARD CJ *et al.*: Peripheral blood gene expression profiling in Sjögren's syndrome. *Genes Immun* 2009; 10: 285-96.
  15. DEVAUCHELLE-PENSEC V, CAGNARD N, PERS JO, YOUINOUP P, SARAUX A, CHIOCHIA G: Gene expression profile in the salivary glands of primary Sjögren's syndrome patients before and after treatment with rituximab. *Arthritis Rheum* 2010; 62: 2262-71.
  16. GREENWELL-WILD T, MOUTSOPOULOS NM, GLIOZZI M *et al.*: Chitinases in the salivary glands and circulation of patients with Sjögren's syndrome: macrophage harbingers of disease severity. *Arthritis Rheum* 2011; 63: 3103-15.
  17. HU S, WANG J, MEIJER J *et al.*: Salivary proteomic and genomic biomarkers for primary Sjögren's syndrome. *Arthritis Rheum* 2007; 56: 3588-600.
  18. PEREZ P, ANAYA JM, AGUILERA S *et al.*: Gene expression and chromosomal location for susceptibility to Sjögren's syndrome. *J Autoimmun* 2009; 33: 99-108.
  19. WANG Z, GERSTEIN M, SNYDER M: RNA-Seq: a revolutionary tool for transcriptomics. *Nat Rev Genet* 2009; 10: 57-63.
  20. LOVE MI, HUBER W, ANDERS S: Moderated estimation of fold change and dispersion for RNA-seq data with DESeq2. *Genome Biol* 2014; 15: 550.
  21. SUBRAMANIAN A, TAMAYO P, MOOTHA VK *et al.*: Gene set enrichment analysis: a knowledge-based approach for interpreting genome-wide expression profiles. *Proc Natl Acad Sci USA* 2005; 102: 15545-50.
  22. LIVAK K, SCHMITTGEN TD: Analysis of relative gene expression data using real-time quantitative PCR and the 2(-Delta Delta C(T)) Method. *Methods* 2001; 25: 402-8.
  23. ROBERTSON D, SAVAGE K, REIS-FILHO JS, ISACKE CM: Multiple immunofluorescence labelling of formalin-fixed paraffin-embedded (FFPE) tissue. *BMC Cell Biol* 2008; 9: 13.
  24. SHI SR, SHI Y, TAYLOR CR: Antigen retrieval immunohistochemistry: review and future prospects in research and diagnosis over two decades. *J Histochem Cytochem* 2011; 59: 13-32.
  25. SZABO K, PAPP G, DEZSO B, ZEHER M: The histopathology of labial salivary glands in primary Sjögren's syndrome: focusing on follicular helper T cells in the inflammatory infiltrates. *Mediators Inflamm* 2014; 2014: 631787.
  26. VOULGARELIS M, TZIOUFAS AG: Current aspects of pathogenesis in Sjögren's syndrome. *Ther Adv Musculoskelet Dis* 2010; 2: 325-34.
  27. OHTANI N, BRENNAN P, GAUBATZ S *et al.*: Epstein-Barr virus LMP1 blocks p16INK4a-RB pathway by promoting nuclear export of E2F4/5. *J Cell Biol* 2003; 162: 173-83.
  28. HAN M, YAN W, GUO W *et al.*: Hepatitis B virus-induced hFGL2 transcription is dependent on c-Ets-2 and MAPK signal pathway. *J Biol Chem* 2008; 283: 32715-29.
  29. PARK US, PARK SK, LEE YI, PARK JG, LEE YI: Hepatitis B virus-X protein upregulates the expression of p21waf1/cip1 and prolongs G1->S transition via a p53-independent pathway in human hepatoma cells. *Oncogene* 2000; 19: 3384-94.
  30. FOX RI, LUPPI M, KANG HI, PISA P: Reactivation of Epstein-Barr virus in Sjögren's syndrome. *Springer Semin Immunopathol* 1991; 13: 217-31.
  31. HARLEY JB, ZOLLER EE: Editorial: What caused all these troubles, anyway? Epstein-Barr virus in Sjögren's syndrome reevaluated. *Arthritis Rheumatol* 2014; 66: 2328-30.
  32. WEN S, SHIMIZU N, YOSHIYAMA H, MIZUGAKI Y, SHINOZAKI F, TAKADA K: Association of Epstein-Barr virus (EBV) with Sjögren's syndrome: differential EBV expression between epithelial cells and lymphocytes in salivary glands. *Am J Pathol* 1996; 149: 1511-7.
  33. MARTIN-FONTECHA A, SEBASTIANI S, HOPKIN UE *et al.*: Regulation of dendritic cell migration to the draining lymph node: impact on T lymphocyte traffic and priming. *J Exp Med* 2003; 198: 615-21.
  34. RIOL-BLANCO L, SANCHEZ-SANCHEZ N, TORRES A *et al.*: The chemokine receptor CCR7 activates in dendritic cells two signaling modules that independently regulate chemotaxis and migratory speed. *J Immunol* 2005; 174: 4070-80.
  35. AVELLA M, LORIOL C, BOULUKOS K, BORGESSE F, EHRENFELD J: SLC26A9 stimulates CFTR expression and function in human bronchial cell lines. *J Cell Physiol* 2011; 226: 212-23.
  36. BERTRAND CA, ZHANG R, PILEWSKI JM, FRIZZELL RA: SLC26A9 is a constitutively active, CFTR-regulated anion conductance in human bronchial epithelia. *J Gen Physiol* 2009; 133: 421-38.
  37. LIU X, LI T, RIEDERER B *et al.*: Loss of SLC26a9 anion transporter alters intestinal electrolyte and HCO<sub>3</sub><sup>-</sup> transport and reduces survival in CFTR-deficient mice. *Pflugers Arch* 2015; 467: 1261-75.
  38. STRUG LJ, GONSKA T, HE G *et al.*: Cystic fibrosis gene modifier SLC26A9 modulates airway response to CFTR-directed therapeutics. *Hum Mol Genet* 2016;
  39. KHUDER SA, AL-HASHIMI I, MUTGI AB, ALTOROK N: Identification of potential genomic biomarkers for Sjögren's syndrome using data pooling of gene expression microarrays. *Rheumatol Int* 2015; 35: 829-36.
  40. SONG GG, KIM JH, SEO YH, CHOI SJ, JI JD, LEE YH: Meta-analysis of differentially expressed genes in primary Sjögren's syndrome by using microarray. *Hum Immunol* 2014; 75: 98-104.
  41. WILDENBERG ME, VAN HELDEN-MEEUWSEN CG, VAN DE MERWE JP, DREXHAGE HA, VERSNEL MA: Systemic increase in type I interferon activity in Sjögren's syndrome: a putative role for plasmacytoid dendritic cells. *Eur J Immunol* 2008; 38: 2024-33.
  42. MAEHARA T, MORIYAMA M, HAYASHIDA JN *et al.*: Selective localization of T helper subsets in labial salivary glands from primary Sjögren's syndrome patients. *Clin Exp Immunol* 2012; 169: 89-99.
  43. CARUBBI F, ALUNNO A, CIPRIANI P *et al.*: Is minor salivary gland biopsy more than a diagnostic tool in primary Sjögren's syndrome? Association between clinical, histopathological, and molecular features: a retrospective study. *Semin Arthritis Rheum* 2014; 44: 314-24.
  44. LEE KE, KANG JH, YIM YR *et al.*: Predictive significance of CCL21 and CXCL13 levels in the minor salivary glands of patients with Sjögren's syndrome. *Clin Exp Rheumatol* 2017; 35: 234-40.
  45. BARRERA MJ, BAHAMONDES V, SEPULVEDA D *et al.*: Sjögren's syndrome and the epithelial target: a comprehensive review. *J Autoimmun* 2013; 42: 7-18.
  46. KONTTINEN YT, HALINEN S, HANEMAAIJER R *et al.*: Matrix metalloproteinase (MMP)-9 type IV collagenase/gelatinase implicated in the pathogenesis of Sjögren's syndrome. *Matrix Biol* 1998; 17: 335-47.
  47. GOICOVICH E, MOLINA C, PEREZ P *et al.*: Enhanced degradation of proteins of the basal lamina and stroma by matrix metalloproteinases from the salivary glands of Sjögren's syndrome patients: correlation with reduced structural integrity of acini and ducts. *Arthritis Rheum* 2003; 48: 2573-84.
  48. PEDERSEN AM, BARDOW A, NAUNTOFTE B: Salivary changes and dental caries as potential oral markers of autoimmune salivary gland dysfunction in primary Sjögren's syndrome. *BMC Clin Pathol* 2005; 5: 4.
  49. PIJPE J, KALK WW, BOOTSMAN H, SPIJKERKOVET FK, KALLENBERG CG, VISSINK A: Progression of salivary gland dysfunction in patients with Sjögren's syndrome. *Ann Rheum Dis* 2007; 66: 107-12.